Hydrological controls on diurnal ice flow variability in valley glaciers

P. W. Nienow,[1] A. L. Hubbard,[1] B. P. Hubbard,[2] D. M. Chandler,[2] D. W. F. Mair,[3] M. J. Sharp,[4] and I. C. Willis[5]

Received 24 November 2004; revised 3 April 2005; accepted 16 June 2005; published XX Month 2005.

[1] This paper uses a combination of field data and three-dimensional modeling to investigate the spatial variability in basal conditions required to induce observed fluctuations in diurnal ice velocity at Haut Glacier d'Arolla, Switzerland. A network of surface velocity markers was observed at intervals of as little as four hours over diurnal cycles in both winter and late summer. Winter motion showed limited diurnal variability, presumably due to the absence of supraglacial meltwater inputs. By contrast, diurnal fluctuations in ice motion were recorded in summer across the lower and upper glacier. In the lower glacier, surface velocities were intimately linked to hydrological forcing in the vicinity of a subglacial channel. Previously observed diurnal excursions of meltwater away from the channel should reduce areas of basal drag adjacent to the channel thereby impacting on ice dynamics. Using a first-order ice flow approximation, we investigated the distribution of basal shear traction adjacent to the channel necessary to replicate the observed surface velocity field during periods of rapid ice motion. The modeling suggests that the observed variations in diurnal velocity will only occur with extensive reductions in basal drag across a transverse zone of up to 560 m across, well beyond the immediate vicinity and previously observed extent of diurnal excursions of meltwater away from the subglacial channel.

Citation: Nienow, P. W., A. L. Hubbard, B. P. Hubbard, D. M. Chandler, D. W. F. Mair, M. J. Sharp, and I. C. Willis (2005), Hydrological controls on diurnal ice flow variability in valley glaciers, *J. Geophys. Res.*, *110*, XXXXXX, doi:10.1029/2003JF000112.

1. Introduction

[2] Ice flow velocities at individual ice masses can fluctuate over a variety of spatial and temporal scales. The conditions at the ice-bed interface that result in transient speedup events such as glacier surges [*Raymond*, 1987] and spring events [*Iken et al.*, 1983] may vary but it is generally assumed that speedups result from enhanced basal motion. While areas of high basal water pressure/low drag are required to initiate enhanced basal motion, the actual basal configurations necessary to induce such velocity perturbations are unclear [*Blatter et al.*, 1998]. Furthermore, the presence of sticky/slippery spots is also likely to play a critical role in sliding [*Fischer and Clarke*, 1997]. However, the length scales (both longitudinal and transverse) over which such variations in basal drag must occur to cause widespread motion remain poorly understood [*Harbor et al.*, 1997]. In addition, the extent to which reduced drag in one zone can induce a speedup response in adjacent areas as a result of longitudinal and transverse coupling is also unclear.

[3] From a theoretical perspective, *Balise and Raymond* [1985] used an analytical model to examine the transfer of basal velocity anomalies to the surface of a planar parallel-sided slab of linear viscous rheology. They identify four contrasting scales of behavior-dependent on the length of the applied basal velocity anomaly. At very short scales of less than ice thickness (H) they essentially found no response at the glacier surface. They found that at scales of between 1 and 5H the surface response was of up to 0.3 of the applied horizontal basal velocity anomaly and at intermediate scales between 5H and 10H the surface response was not only further amplified but also significantly attenuated beyond the area above the applied basal anomaly. Finally, at long scales, greater than 10H, the response at the surface was essentially the same as the applied anomaly at the bed with little spatial attenuation.

[4] These findings are supported by the work of *Blatter et al.* [1998], who used a numerical model identical to that applied in this paper but limited to two dimensions (in longitudinal section) to investigate the changing length scale of a basal perturbation on an idealized homogeneous nonsliding slab. They found that through introducing an isolated slippery zone of zero basal shear traction, not only

[1]School of Geosciences, University of Edinburgh, Edinburgh, UK.
[2]Centre for Glaciology, Institute of Earth Studies, University of Wales, Aberystwyth, UK.
[3]Department of Geography and Environment, University of Aberdeen, Aberdeen, UK.
[4]Department of Earth and Atmospheric Sciences, University of Alberta, Edmonton, Alberta, Canada.
[5]Department of Geography, University of Cambridge, Cambridge, UK.

0148-0227/05/2003JF000112$09.00

does the magnitude of the glacier response directly relate to the area of zero traction but the computed basal velocity within this zone is limited and determined by nonlocal variables. Even with decoupling of the ice from the bed over a zone of $\sim 5H$, they found that sliding velocity remains strongly limited by longitudinal stress gradients and that local stress reduction is accompanied by a concentration of traction up and down glacier. On application of this flow line model to the geometry of Haut Glacier d'Arolla with a 300 m zone of imposed zero basal shear traction, they found surface velocities increase by some 100% over the basal perturbation and that the surface response extended some 500 m down glacier and 1000 m up glacier. *Blatter et al.* [1998] conclude with a rejection of a sliding law based on strictly local variables such as the driving stress in favor of a nonlocal treatment that includes longitudinal stresses and takes basal velocity to be an integrated response to spatially varying influences. These findings resonate with the previous work of *Echelmeyer and Kamb* [1986], who investigated the coupling effects of longitudinal stress gradients on glacier flow using theoretical considerations and flow data from Blue Glacier, Washington. In an attempt to further improve on this understanding of how nonuniform bed conditions affect glacier dynamics, this paper uses a combination of field data and a three-dimensional version of the *Blatter et al.* [1998] model to investigate the spatial extent of reductions in basal drag required to induce the observed subdiurnal fluctuations in velocity at Haut Glacier d'Arolla.

[5] Diurnal variations in glacier velocity have been observed at many glaciers (both temperate and polythermal), but not all glaciers show diurnal cyclicity [*Iken*, 1974]. In general, diurnal velocity cycles are most likely on days with pronounced diurnal meltwater inputs, whereby peaked supraglacial meltwater inputs to the subglacial drainage system result in high basal water pressures and associated periods of rapid basal motion [*Iken and Bindschadler*, 1986]. The area over which basal water pressures are perturbed will be dependent on the configuration of the subglacial drainage system and the flux of meltwater delivered to the system [*Kamb*, 1987]. In a channelized system, rapid increases in water flux through the channel may result in a rise in within-channel pressure sufficient to generate a pressure gradient directed away from the channel. Under such conditions (such as during a rapidly rising discharge hydrograph due to rainfall or surface melt), excursions of meltwater away from the channel will occur [*Hubbard et al.*, 1995] thereby reducing effective pressure along a longitudinal section of the bed adjacent to the subglacial channel. The overall impact of such excursions on coupling at the ice-bed interface will depend on the number and spacing of subglacial channels and the pressure perturbations within them (which will depend on their shape [*Hooke et al.*, 1990] and the rate of change of discharge through each channel). In addition, any decrease in effective pressure adjacent to the channels will transfer stresses to the interchannel areas potentially modifying rates of basal motion across large areas of the bed [*Harbor et al.*, 1997; *Gordon et al.*, 1998]. While diurnal variations in glacier motion have been observed at many glaciers, the potential role of meltwaters driven laterally away from subglacial channels in causing such variations has not been investigated.

2. Rationale

[6] Previous investigations of borehole water levels in the vicinity of a subglacial channel at Haut Glacier d'Arolla, Switzerland, indicated that channel water pressures regularly rose above overburden pressure during diurnal cycles in mid-late summer due to highly peaked supraglacial meltwater inputs [*Hubbard et al.*, 1995]. The resulting pressure gradient drove meltwaters away from the channel transverse to ice flow over a lateral distance of about 70 m (across a zone which Hubbard et al. termed the variable pressure axis or VPA). Such a transfer of water will clearly result in a change in the local basal stress configuration in the vicinity of the channel (with basal drag being at a minimum closest to the channel) [*Gordon et al.*, 1998]. Any decrease in the basal drag may affect ice dynamics, since lateral diurnal variations in water flow will result in systematic variations in subglacial water pressures [*Hubbard et al.*, 1995]. In order to explore this possibility, this paper investigates the incidence of diurnal variations in glacier velocity at Haut Glacier d'Arolla, Switzerland. More specifically, the paper aims to (1) determine whether diurnal velocity fluctuations, if observed, are both spatially limited to areas immediately adjacent to subglacial channels and temporally controlled by diurnal excursions of water from these channels and (2) determine using modeling, how local reductions in basal drag in the vicinity of subglacial channels impacts on glacier dynamics as a result of coupling via longitudinal and transverse stress gradients.

3. Field Site

[7] Haut Glacier d'Arolla, Switzerland, is a 4 km long, temperate valley glacier with a maximum thickness in 1990 of about 180 m [*Sharp et al.*, 1993] (Figure 1). Extensive investigations of the glacier's hydrology and dynamics have been undertaken since 1989 and detailed discussions of the field and modeling results can be found elsewhere [e.g., *Richards et al.*, 1996; *Nienow et al.*, 1998; *Hubbard et al.*, 1998]. Of particular relevance to this paper are the subglacial drainage conditions outlined below.

3.1. Subglacial Hydrology at Haut Glacier d'Arolla

[8] Evidence from a variety of field data (dye and borehole investigations) suggests that for much of the summer, most supraglacially derived meltwaters are routed under the main glacier tongue by a hydraulically efficient channelized system [*Hubbard et al.*, 1995; *Nienow et al.*, 1998]. This channelized system (or "fast" subsystem [*Raymond* et al., 1995]) expands upglacier over the course of the melt season at the expense of a hydraulically inefficient distributed system (or "slow" subsystem [*Raymond* et al., 1995]) which remains between the subglacial channels. In addition, the distributed drainage system remains beneath the uppermost 0.7 km of the glacier [*Nienow et al.*, 1998]. Theoretical predictions of subglacial channel patterns in conjunction with dye returns suggests that the glacier tongue is drained by two main channels [*Sharp et al.*, 1993] (Figure 1), the existence of one of which (the easterly) has been confirmed

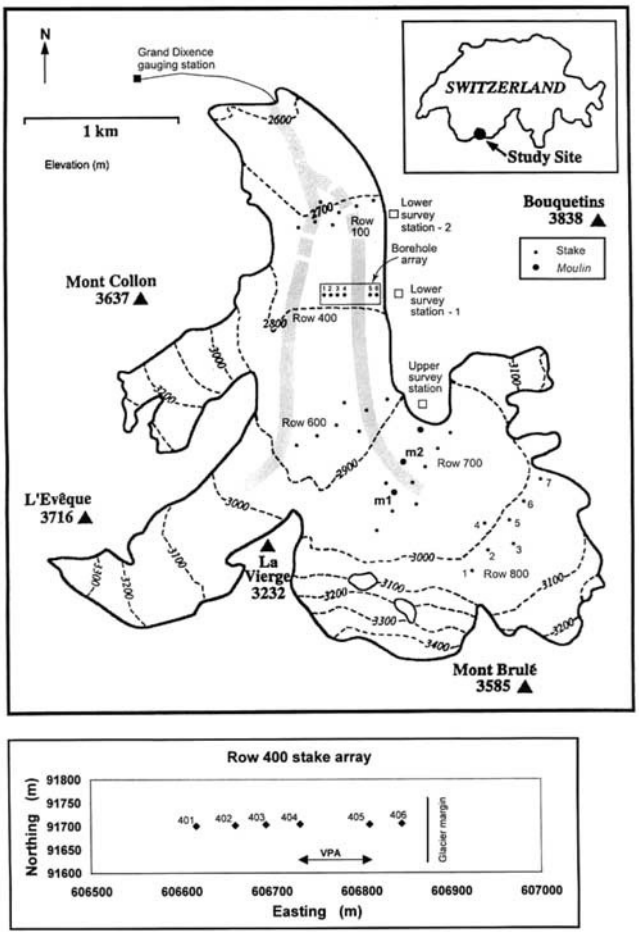

Figure 1. Map of Haut Glacier d'Arolla (latitude 46°0′N, longitude 7°30′E), showing positions of the stake arrays, survey stations, moulins referred to in the text, and the position and extent of the variable pressure axis (VPA) identified from borehole investigations [*Hubbard et al.*, 1995]. The gray shading shows the location of the primary subglacial drainage paths as predicted from the subglacial hydraulic potential surface and dye tracing tests [*Sharp et al.*, 1993].

by an intensive borehole drilling program between 1992 and 2000 [*Hubbard et al.*, 1995; *Gordon et al.*, 1998; *Mair et al.*, 2003]. Water pressure records from the boreholes indicate that the position of the easterly channel has been stable between years and dye tracer tests over eight summers between 1989 and 2000 confirm that the channel provides a hydraulically efficient "fast" route for the drainage of meltwaters by August each year.

[9] As noted above, the eastern channel experiences significant diurnal water pressure variations driven by supraglacial meltwater inputs, whereby diurnally reversing, transverse hydraulic gradients drive water away from the channel into the distributed system during the late morning/afternoon and back to the channel overnight. During August 1993, water levels in boreholes near the channel rose most rapidly between 1130 and 1400 LT and about 2 hours later at boreholes located 20 m from the channel and water pressures typically peaked near the center of the VPA at around 1700 LT [*Hubbard et al.*, 1995] (Figure 2). These observations are characteristic of late summer fluctuations in borehole water pressures in the vicinity of the VPA although these investigations have only been undertaken in a narrow zone on the eastern side of the glacier 1.5 km above the terminus (Figure 1). The extent to which water pressure fluctuations observed in this area are characteristic of areas adjacent to channels elsewhere beneath the glacier is unknown. However, evidence from dye tracing experiments indicates that surface meltwaters flow through pressurized tributary channels prior to draining into the two main subglacial paths [*Nienow et al.*, 1996]. In addition, records of moulin water levels during August 1990 and 1991 indicated that levels regularly reached heights above overburden at sites m1 and m2 located further upglacier (Figure 1) [*Nienow*, 1993]. Peaks in moulin water level typically occurred between 1400 and 2000 LT and remained close to overburden pressure for 2–5 hours. The occurrence and characteristics of these diurnal fluctuations in water level are similar to those recorded at other glaciers [e.g., *Holmlund and Hooke*, 1983].

3.2. Surface Motion

[10] Between 1994 and 1996, networks of velocity markers were drilled into the glacier surface and ice velocity data were obtained at a variety of timescales by standard ground surveying using a Geotronics Geodimeter 410 total station. Information on annual, intra-annual and seasonal flow characteristics are reported elsewhere [*Harbor et al.*, 1997; *Hubbard et al.*, 1998; *Mair et al.*, 2001]. In this paper, measurements of ice motion at arrays 800 in the upper glacier and 400 in the lower glacier are presented to

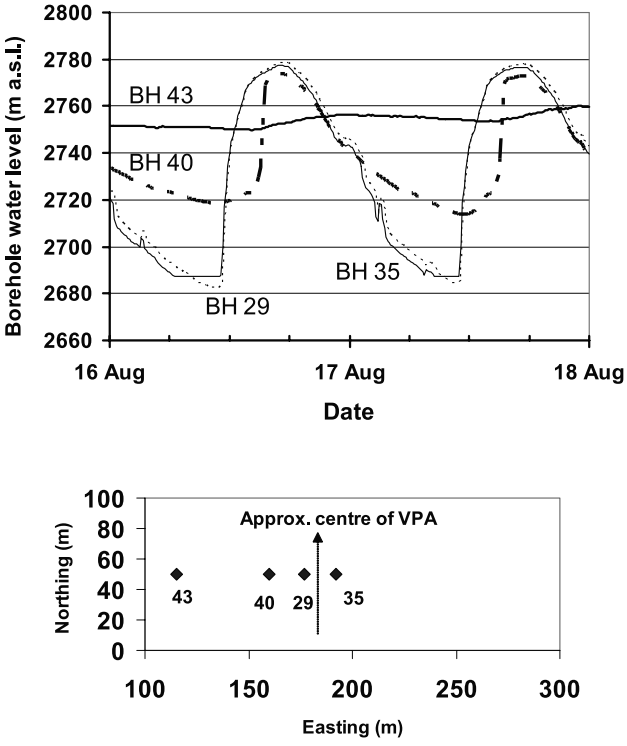

Figure 2. Water level time series recorded in boreholes located transverse to the variable pressure axis (VPA) on 16–17 August 1993. The positions of the boreholes relative to the VPA are shown.

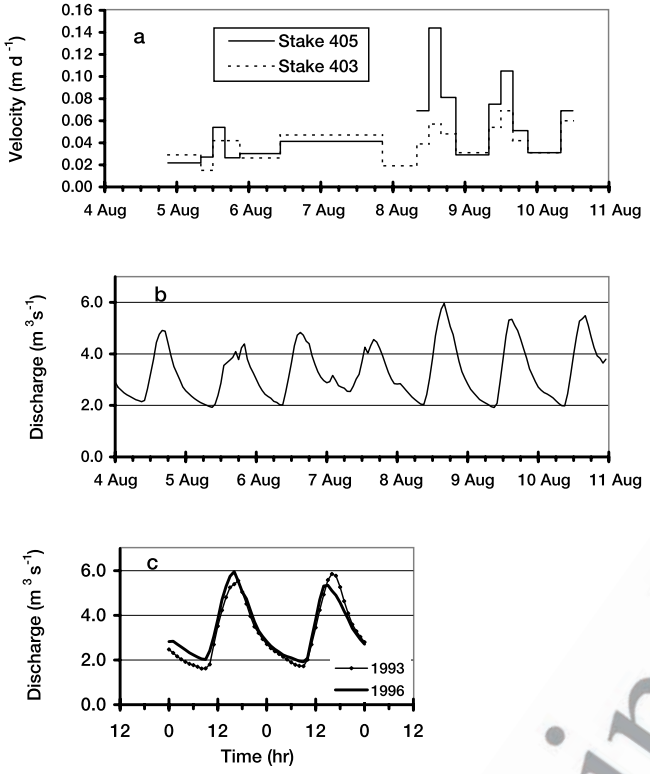

Figure 3. Temporal record of (a) horizontal velocities at stakes 403 and 405 and (b) proglacial stream discharge between 4 and 10 August 1996. Error estimates vary between 0.004, 0.012, and 0.024 m d^{-1} during 24, 12, and 4 hour survey periods, respectively. (c) Proglacial stream discharge on 16–17 August 1993 and 8–9 August 1996.

illustrate variations in subdiurnal flow characteristics (Figure 1). These rows are selected since (1) row 400 is located in the vicinity of the borehole array where water pressure fluctuations have been repeatedly observed between 1992 and 2000 and (2) during mid-late summer, they typically overlie areas of the bed with different subglacial drainage configurations (channelized and distributed below rows 400 and 800, respectively [*Nienow et al.*, 1998]) which may result in different motion characteristics.

[11] The stakes in arrays 400 and 800 were surveyed at intervals of as little as four hours during both summer and winter in order to investigate subdiurnal flow variability. Row 800 was surveyed at this detail on 11 and 12 July 1994 and 6–9 February 1995 and row 400 was surveyed between 27 and 31 January and between 4 and 10 August 1996. All stakes within each array were surveyed twice during each survey and reference targets were established on bedrock and repeatedly surveyed to reduce errors (see *Mair et al.* [2001] for fuller details). The rated accuracy of the survey station and the refraction error of the prisms meant the stake positions could be determined with an accuracy of ±4–5 mm over the range of distances surveyed.

4. Results

4.1. Lower Glacier Velocities

[12] Horizontal velocities from two stakes in row 400 between 4 and 10 August demonstrate clear variations in flow velocity over a diurnal cycle (Figure 3a). The temporal behavior of the selected stakes is broadly representative of stakes across array 400 during the survey period, although individual velocities and magnitudes of change vary between stakes (see below). During the periods of most frequent surveys (4–6 August and 8–10 August), velocities were typically lowest overnight between 2000 and 0800 LT, increased between 0800 and 1200 LT and peaked between 1200 and 1600 LT with peaks reaching 2–6 times overnight velocities (Figure 4a). Overnight velocities (2000–0800 LT) decrease from 0.032 m d^{-1} at stake 401 near the glacier centerline to 0.020m d^{-1} near the glacier margin at stake 406. Mean daily velocities show a similar pattern but are slightly higher while winter velocities are lower. Velocities between 1200 and 1600 LT are significantly higher but the general decrease in velocity toward the glacier margin is interrupted by a clear velocity enhancement at stakes 404 and 405. A more detailed breakdown shows that velocities at stakes away from the VPA are lower between 0800 and 1200 LT than between

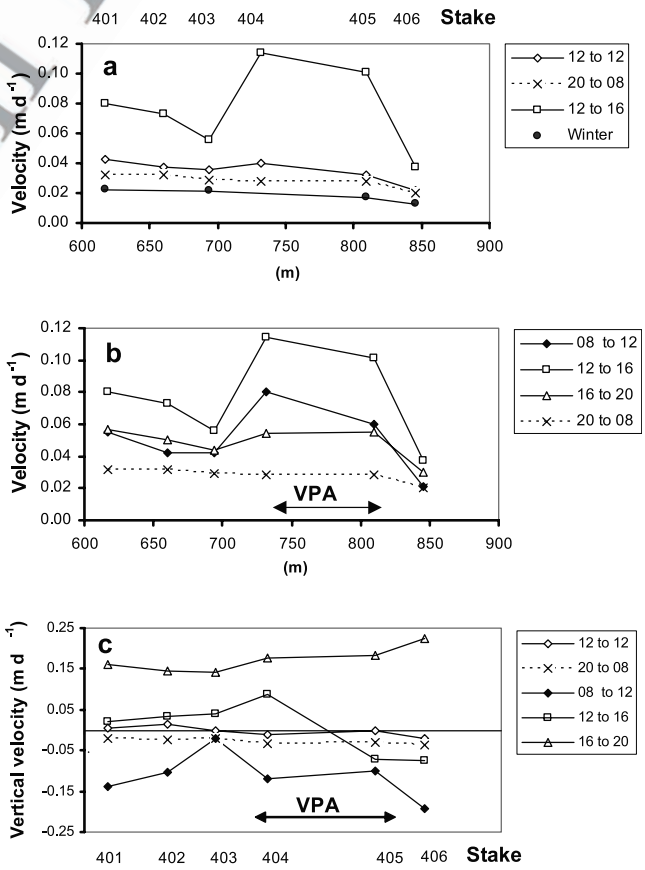

Figure 4. (a and b) Mean horizontal and (c) vertical velocities at stakes in array 400 for different temporal intervals between 4 and 10 August 1996. Velocity errors vary between 0.004, 0.012, and 0.024 m d^{-1} during 24, 12, and 4 hour survey periods, respectively. The *x* axis in m represents the last three digits of the Swiss grid easting and full values start with 606. (Numbers in legend refer to time in hours, i.e., 12 to 12 represents 1200 to 1200 LT 24 hour period; 20 to 08 represents 2000 to 0800 LT 12 hour period).

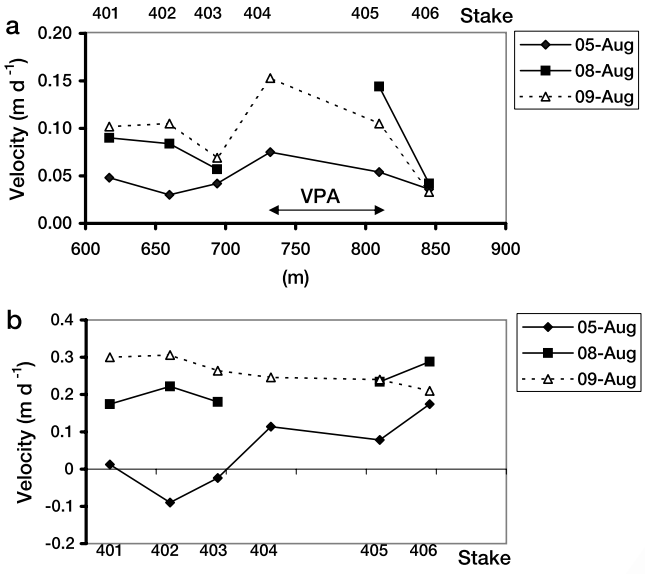

Figure 5. Mean (a) horizontal velocities between 1200 and 1600 and (b) vertical velocities between 1600 and 2000 LT at stakes in array 400 on 5, 8, and 9 August 1996, respectively.

1600 and 2000 LT, while the reverse is true at stakes 404 and 405 (Figure 4b).

[13] Mean vertical velocities in row 400 reveal highest positive velocities (i.e., uplift) between 1600 and 2000 LT with rates across the array being relatively constant between 0.14 and 0.22 m d^{-1} (Figure 4c). Vertical velocities increase during the day to the 1600–2000 LT peak following highest negative velocities (i.e., surface lowering) between 0800 and 1200 LT. However, while vertical velocities at stakes 401–404 become positive between 1200 and 1600 LT, they remain negative at stakes 405–406 near the eastern glacier margin.

[14] It is clear from Figure 3a that velocities at the same stake during the same period of a diurnal cycle (e.g., 1200–1600 LT) can vary between days. Such variability is highlighted in Figure 5a whereby flow velocities between 1200 and 1600 LT are, with the exception of stake 406, between 1.5 and 2 times faster on 8 and 9 August compared with 5 August. The vertical velocities between 1600 and 2000 LT also demonstrate higher rates of uplift on 8 and 9 August than on 5 August (Figure 5b).

4.2. Upper Glacier Velocities

[15] As in the lower glacier, horizontal velocities in row 800 show diurnal variability in summer flow velocities during the period 10–13 July (Figures 6a and 6b). However, in the upper glacier, velocities reach maxima between 1700 and 2100 LT with flow velocities at a minimum between 0900 and 1300 LT (Figure 7). The velocities show a general asymmetry across the array and decrease from south (stake 801) to north (stake 806) across the glacier. In contrast to summer velocities, winter motion is virtually constant over a diurnal cycle (Figure 6c).

5. Interpretation of Results

5.1. Lower Glacier

[16] During summer, horizontal and vertical velocities show considerable variability over diurnal cycles (Figure 4). Across array 400, mean summer and winter velocities show a general decrease from the glacier center to the margin as expected in response to decreasing ice thickness (and thus deformation) (Figure 4a). Minimum summer velocities between 2000 and 0800 LT are still faster than winter velocities likely suggesting a sliding component in summer. While maximum velocities at all stakes between 1200 and 1600 LT suggest increased rates of basal sliding, the velocity enhancement at stakes 404 and 405 (located above the VPA) is much greater than elsewhere. This

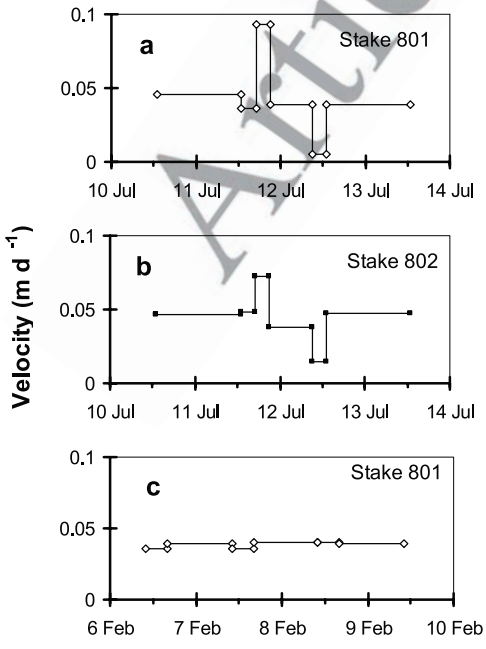

Figure 6. Temporal record of horizontal velocities at stakes (a) 801 and (b) 802 between 10 and 14 July 1994 and (c) 801 between 6 and 9 February 1995. Velocity errors vary between 0.005 and 0.030 m d^{-1} during 24 and 4 hour survey periods, respectively.

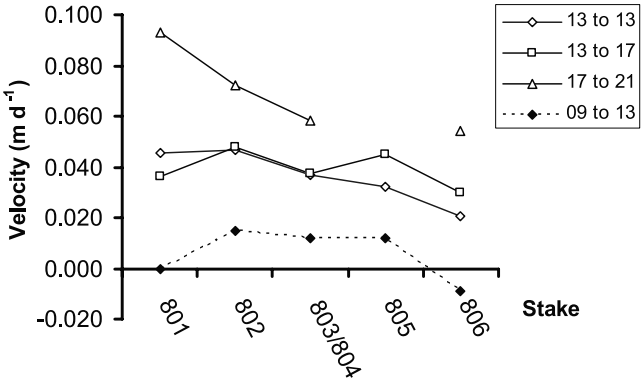

Figure 7. Horizontal velocities at stakes in row 800 for different temporal intervals between 11 and 12 July 1994. Velocity errors vary between 0.005 and 0.030 m d^{-1} during 24 and 4 hour survey periods, respectively.

suggests that a decrease in basal drag in the immediate vicinity of the VPA is driven by water inputs to the VPA from supraglacial sources upglacier. The fact that the highest velocities occur between 1200 and 1600 LT (as opposed to 1600 and 2000 LT) suggests that reduction in basal drag is not precisely correlated with water pressure which is higher on average during the later period (Figure 2) [*Hubbard et al.*, 1995]. (The similarity in timing and magnitude of discharge during the water pressure record (1993) and velocity record (1996) suggest that the timing of water pressure variations within the VPA was very similar in 1993 and 1996 (Figure 3c).) Instead, the data show that maximum velocities occurred when water pressures were rising rather than at their peak. These findings match previous field observations [*Fischer and Clarke*, 1997] and replicate *Iken*'s [1981] modeling of the effect of subglacial water pressure on sliding velocity. We appeal to *Fischer and Clarke*'s [1997, p. 390] concept of a stick-slip mechanism to explain our results whereby "as the water pressure rises, a local strain build-up in the ice is released, resulting in a momentary increase in sliding rate; once the finite relaxation has occurred, further rises in water pressure do not produce additional enhancement of basal sliding." We suggest that the diurnal excursions of meltwater away from the channel and associated increase in basal water pressures result in a critical bed separation threshold whereby basal drag is reduced and the glacier speeds up. The diurnal speedups may reflect the gradual failure of a "sticky spot" following hydraulic connection of areas adjacent to the channel and resultant changes in basal drag [*Kavanaugh and Clarke*, 2001].

[17] While horizontal velocities are most rapid between 1200 and 1600 LT, maximum rates of vertical uplift (Z velocity) occurred between 1600 and 2000 LT (Figure 4c). A detailed analysis is required to determine the extent to which such uplift is caused by strain events, water storage or both [*Gudmundsson et al.*, 1997]. Unfortunately, the data required to determine the precise contribution of vertical extension to this positive vertical component are unavailable. However, estimates of vertical straining in the same area of the glacier by *Mair et al.* [2002] demonstrate that bed separation is occurring when the observed vertical velocities are considerably lower than we observe here. It thus seems likely that some of the uplift is the result of bed separation. If bed separation is occurring, this indicates that a critical threshold in the reduction of basal drag is reached between 1200 and 1600 LT and subsequent bed separation does not enhance rates of basal sliding.

[18] Higher horizontal and vertical velocities on 8 and 9 August than on 5 August are consistent with variations in the amplitude of the discharge hydrograph which was more subdued under cloudy conditions on 5 August (Figure 3b). Discharge on 5 August peaked at 4.39 $m^3\ s^{-1}$ (2.3 times the 10.00 minimum discharge) while discharges on 8 and 9 August peaked at 5.96 and 5.35 $m^3\ s^{-1}$, respectively (with increases of 2.9 and 2.8 times the 10.00 minimum). The higher discharges on 8 and 9 August are clearly likely to result in both higher and more laterally extensive water pressure perturbations away from the VPA with an associated decrease in basal drag and increase in ice motion. Numerous earlier studies have demonstrated a similar correlation between patterns of meltwater input to the glacier and glacier surface velocity [*Willis*, 1995].

5.2. Upper Glacier

[19] While summer velocities in the upper glacier show clear diurnal variability (Figure 7), the results at row 800 differ from those in the lower glacier in the following key respects.

[20] 1. Maximum velocities in row 800 occurred later in the diurnal cycle between 1700 and 2100 LT. This is likely the result of both the thick snowpack and firn layer in the vicinity of row 800 in mid-July 1994 which would delay inputs of meltwater into the subglacial system. Peak proglacial discharges occurred 1–3 hours later during the July surveys than during those in August 1996 reflecting the impact of the snowpack on the timing of the diurnal runoff peak.

[21] 2. The array in row 800 showed no evidence of any localized velocity enhancement above an apparent conduit. Since dye tracing work over several melt seasons suggests this area is typically underlain by a distributed drainage system in July, meltwater inputs to such a system would be expected to perturb the basal water pressures across a more extensive area than under circumstances where water is preferentially routed through large subglacial channels. (The slight asymmetry in flow velocities across the stake array (Figure 7) results from the steeper surface profile on the south of the glacier and from the flow of ice into the main glacier from the ice falls coming off Mont Brulé (Figure 1).)

6. Modeling

[22] The field data presented imply that supraglacially driven hydrological forcing results in areas of high basal water pressure/low drag which initiate enhanced basal motion. This proposition can be tested using a suitably equipped three-dimensional model which calculates the internal stress and velocity fields for given basal velocity and traction distributions. Here, we use the *Blatter* [1995] first-order numerical solution of the mass and force balance equations and constitutive relation for three-dimensional grounded ice masses in steady state to investigate the possible basal drag configurations that could in principle cause the observed diurnal velocity variations.

[23] Specific model derivation, numerical implementation and proof through comparison with an idealized case solution are given by *Blatter* [1995], *Colinge and Blatter* [1998] and *Blatter et al.* [1998]. The model calculates normal deviatoric stresses and lateral shear stresses, handles a nonlinear constitutive relation and calculates the steady state stress and velocity fields for any basal boundary configuration provided by either a velocity or shear traction distribution or a combination of the two. A constitutive relation approximating Glen's flow law is used, which relates the strain rate tensor (D) to the stress deviator ($\sum$):

$$D = A(I_{\mathrm{II}} + t_0)^{(n1)/2} \sum$$

where A is the ice softness, I_{II} is the second invariant of the stress deviator ($\sum$), and n is the flow law exponent taken as 3; t_0 is a nominally small constant of 0.1 bar^2 so as to maintain close resemblance to Glen's flow law while

ensuring a finite viscosity in the limit of zero stress [*Blatter*, 1995]. A is primarily a function of temperature but is also affected by other factors such as ice impurities and water content. Here A is taken as constant and equal to 0.063 yr^{-1} bar^{-3} on the basis of tuning this same model to surface and englacial strain measurements at Haut Glacier d'Arolla taken in 1994–1995 [*Hubbard et al.*, 1998].

[24] *Blatter* [1995] introduces a scaling analysis based on the aspect ratio, ε of the ice mass such that $\varepsilon = \{H\}/\{L\}$, where $\{H\}$ and $\{L\}$ are the vertical and horizontal extents of the ice mass, respectively. For ice sheets and low gradient glaciers, ε is small and allows the definition of a hierarchy of terms in the mass and force balance equations and the constitutive relation based on powers of ε. What *Blatter* [1995] refers to as the first-order approximation is the solution in which terms of order ε^2 and higher are eliminated, to yield five ordinary differential equations and three algebraic equations. These can be solved numerically for any given three-dimensional ice mass geometry.

[25] Starting with the specified basal boundary condition and an estimate for the unknown basal shear traction or velocity, the model shoots vertically from the bed to the surface using a second-order Runge-Kutta integration scheme and a root solver. Since the surface boundary condition (zero surface-parallel shear traction) is not automatically satisfied, the unknown basal shear traction or velocity is subsequently modified in an iteration scheme based on the calculated surface shear traction. Convergence is achieved when this computed surface shear traction vanishes to some sufficiently small value (i.e.,<0.0001 bar). The modeling here was undertaken using this first-order algorithm as adapted and successfully applied to Haut Glacier d'Arolla by *Hubbard et al.* [1998] at 70 m horizontal resolution. However, an important difference here compared to the original application, is that the model is improved to handle a mixed basal boundary condition as described by *Colinge and Blatter* [1998, section 2]. The advantage is that this model can be used to investigate the spatial interaction of slip/stick patchiness since a low or zero basal shear traction can be specified to replicate areas of low drag and decoupled zones of the bed while zero sliding can be prescribed over remaining areas to simulate "sticky" basal conditions [*Blatter et al.*, 1998]. In all other aspects the application of the model to the geometry of Haut Glacier d'Arolla is identical to that described by *Hubbard et al.* [1998]. The modeling presented here is specifically intended as a three-dimensional case study extension of *Blatter et al.* [1998] and *Colinge and Blatter* [1998]. These papers technically establish the first-order solution used here and apply it in plane strain under a variety of basal conditions to both idealized and real glacier configurations to explore the efficacy of the schemes and to investigate the effects of basal decoupling on the resulting patterns of stress and velocity at a variety of scales.

[26] The first model experiment (model 1) investigates the effect of locally reducing basal shear traction over a zone either side of the two main channel paths inferred by *Sharp et al.* [1993] (Figure 1). Since the aim is to replicate the basal conditions for the observed speedup, peak subglacial water pressures recorded by *Hubbard et al.* [1995] (Figure 2) were identified to determine the pattern of imposed basal drag. Zero traction ($\tau_b = 0$) was specified in a zone above the channel, where midafternoon basal water pressure exceeds ice overburden pressure. An intermediate value ($\tau_b = 0.24$ bar) at grid points adjacent to the channel axis was chosen based on a reduction in mean basal shear traction as indicated by the pressure record. This spatial configuration of basal shear traction was extended from 0.8 to 2.2 km upglacier from the terminus, along the two drainage channels identified by *Sharp et al.* [1993], and zero sliding was prescribed over the remainder of the bed to yield the mixed basal boundary condition for model 1 (Figure 8c). With respect to the performance and applicability of the model under this basal configuration, *Colinge and Blatter* [1998, section 3] demonstrate that the first-order approximation is quite capable of dealing with such an abrupt transition from no slip to zero traction across a single grid cell. The transition in the model used in the present study is further dampened by the intermediate zone of reduced basal shear traction immediately surrounding the area of zero traction.

[27] The results of model 1 are shown as modeled basal shear traction outside the areas of reduced/zero drag (Figure 8c) and modeled surface velocity in planform (Figure 8d) and in cross section at row 400 (Figure 9). Reducing drag along the channel paths results in the reorganization of the localized pattern of basal drag, to maintain the overall force balance. In particular, substantial increases in basal shear traction of up to 100% compared to the no-sliding case (Figure 8a) occur in areas adjacent to the channels. Despite this, the overall impact on surface velocity results in maximum speeds over the channels of about 20 m yr^{-1} (Figure 9). While this represents a ~175% enhancement over winter velocities (Figures 8b and 9), it is clear that these modeled velocities are significantly lower than the pattern of peak velocities of ~40 m yr^{-1} (~0.11 m d^{-1}) observed over the channel between 1200 and 1600 LT on a diurnal basis (Figures 4a and 9).

[28] The basal boundary condition was therefore incrementally adjusted (model 2) by extending the zone of intermediate drag (i.e., by reducing basal shear traction to the off-channel value of 0.24 bar) over an increased area of the bed transverse to the two main channel paths until modeled velocities matched the magnitude of those observed at stakes 404 and 405 between 1200 and 1600 LT. Figure 8e shows the result of this experiment (model 2) and the extensive area of reduced drag necessary to replicate the peak subdiurnal velocities observed on 8 and 9 August in row 400 together with the modeled basal shear traction (across the nonsliding region) and the resulting surface velocities (Figures 8f and 9, model 2). Model 2 overestimates surface velocities at stakes 401–403 (Figure 9) suggesting that the reduction in basal drag is too great away from the channel. However, increasing the off-channel value of basal shear traction to above 0.24 bar results in underestimation of velocities above the channel at stakes 404 and 405. A model with finer grid spacing than 70 m or a more complex distribution in basal drag is therefore needed to model the velocity profile between 1200 and 1600 LT more accurately.

[29] Results from the modeling indicate that an extensive zone of zero/reduced drag between 280 and 560 m across is required to match the maximum observed surface velocities in row 400. This suggests that diurnal variations in basal

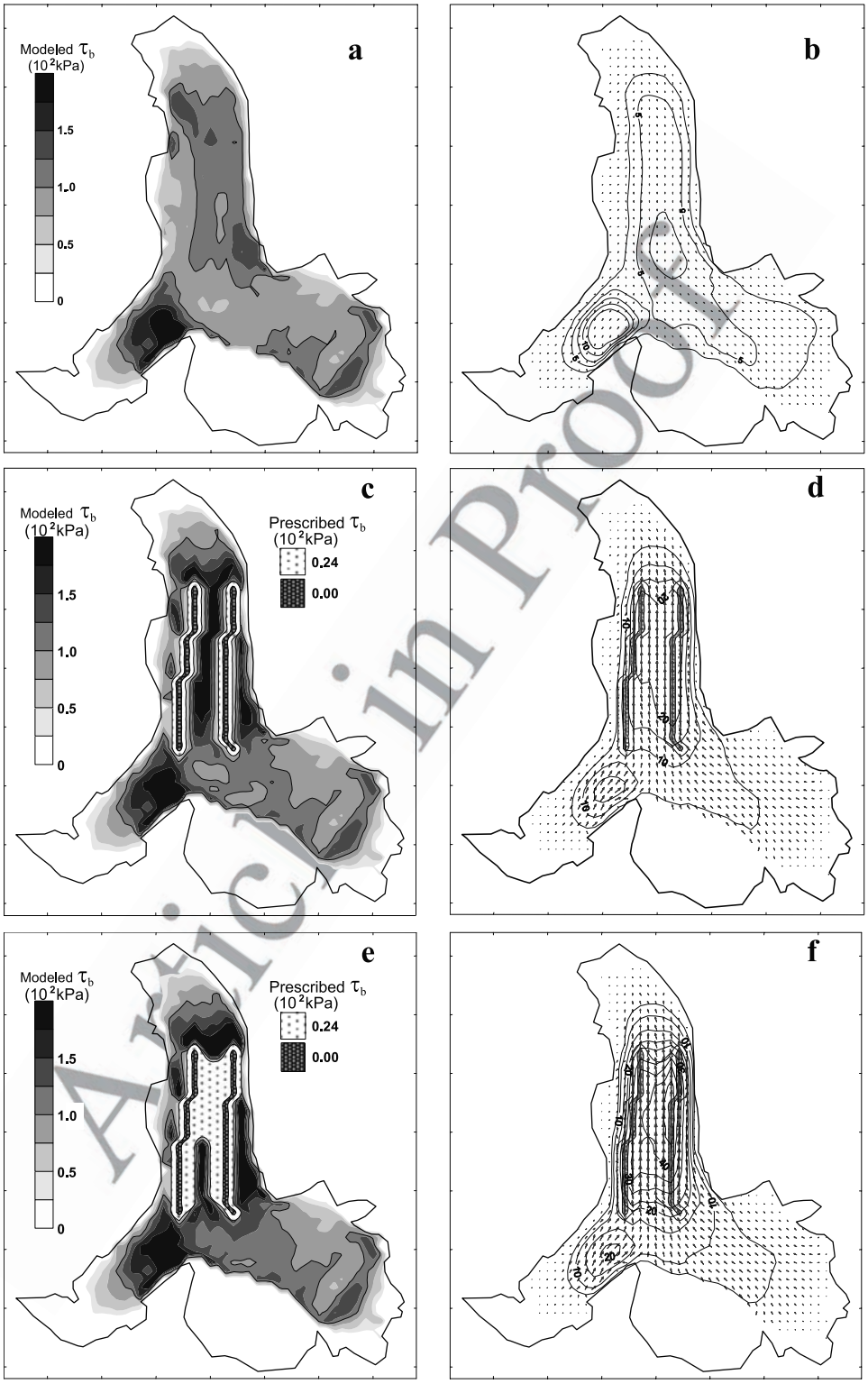

Figure 8. (a, c, and e) Modeled basal shear traction and (b, d, and f) surface velocities in m yr^{-1} resulting from no sliding (Figures 8a and 8b) and reductions in basal drag over prescribed areas of differing spatial extent (speckled shading in Figures 8c and 8e). Figures 8a, 8c, and 8e have a 100 kPa contour line, Figure 8b is contoured at 2.5 m yr^{-1}, and Figures 8d and 8f are contoured at 5 m yr^{-1}.

drag induced by changes in subglacial water pressure must occur in areas considerably more distal to the VPA than was observed in the borehole water levels recorded by *Hubbard et al.* [1995]. Two possible explanations may be invoked to explain this apparent disparity. First, in the absence of borehole water level records, it is possible that the water pressure excursions away from the main channels were simply more extensive in 1996 than those observed in

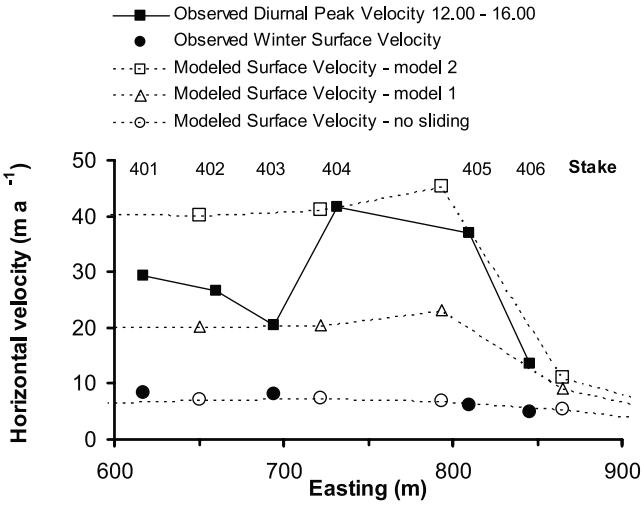

Figure 9. Mean horizontal velocities at stakes in array 400 during winter and peak summer diurnal velocities (4–10 August 1996) and modeled velocities across array 400 under three different modeling scenarios. See text for fuller explanation.

1993. Alternatively, it is likely that tributary subglacial channels feeding into the two main channels also experience high water pressures during peak diurnal discharges thereby resulting in more extensive areas of low basal drag than suggested by the borehole records from 1993. As highlighted earlier, evidence from both dye tracing [*Nienow et al.*, 1996] and moulin water levels [*Nienow*, 1993] suggests that high basal water pressures are likely in areas distal to the main subglacial drainage paths across the lower glacier during times of peak discharge.

7. Discussion and Conclusions

[30] As observed at many other glaciers, Haut Glacier d'Arolla shows clear diurnal velocity variations in summer with minimal variability during winter. The consistently low and invariant winter velocities can be explained by ice deformation alone (Figure 8b), as effectively demonstrated by *Hubbard et al.* [1998]. The summer variability, which is both spatially and temporally complex, is the result of variations in basal motion induced by surface driven hydrological impacts on the spatial pattern of basal drag.

[31] In the lower glacier, in a cross section underlain by a major subglacial channel (termed VPA), surface dynamics are highly sensitive to supraglacial meltwater inputs to this channel and have the following key characteristics:

[32] 1. Maximum horizontal velocities occur between 1200 and 1600 LT during the period of most rapidly increasing basal water pressure as opposed to the time of peak subglacial water pressures (which occur between 1600 and 2000 LT when vertical velocities also peak).

[33] 2. There is an observed velocity peak over the inferred channel, which attenuates away from the channel.

[34] 3. The magnitude of diurnal velocity fluctuations is highly sensitive to day to day variations in supraglacial meltwater inputs to the subglacial drainage system.

[35] In the upper glacier in a region inferred to be overlying a hydraulically distributed subglacial drainage system, summer ice flow is also sensitive to diurnal variations in meltwater input and has the following key characteristics:

[36] 1. Peak horizontal velocities occur between 1700 and 2100 LT, the delay in speedup compared to the lower glacier, likely resulting from the presence of a thick snowpack and firn and an associated delay in the delivery of supraglacially derived meltwaters into the subglacial drainage system.

[37] 2. There is no clear velocity enhancement over a single drainage channel which reflects the more distributed and spatially uniform hydrological conditions in the subglacial drainage system.

[38] Our results provide interesting comparisons with previous investigations of the links between short-term glacier speed up events and hydrology. In particular, the occurrence of maximum velocities during rising water pressures contrasts with many observations where maximum velocities correlate with maximum water pressure [e.g., *Iken and Bindschadler*, 1986; *Jansson*, 1995]. Clearly, individual glaciers will likely behave differently but it is possible, this discrepancy reflects the shorter surveying intervals in our study and that previously derived relationships between water pressure and motion (and sliding laws derived there from) reflect averaged water pressures that do not relate to the precise timing of glacier speedup events. The existence of highly variable water pressures over short temporal (<1 hour) and spatial (<1 ice thickness H) scales also raises concerns that pressure measurements must be obtained from several sites both transverse to and along flow if they are to provide a reliable representation of basal water pressures. Our observations also indicate that the magnitudes of the diurnal speedup events are not directly dependent on the volume of subglacially stored water.

[39] Our results show similarities to the numerical and field results of *Iken* [1981] and *Iken et al.* [1983] where maximum sliding rates coincide with rising water pressure (associated with early stages of cavity growth), not peak water pressure or maximum water storage. However, *Iken et al.* [1983] field observations at Unteraargletscher show highest horizontal velocities correspond to maximum rates of upward ice motion which was not observed at Haut Glacier d'Arolla. We conclude that our observed relationship between changing water pressures and timing of highest velocities likely operates via a "stick-slip" threshold relationship. Thus, as already proposed by *Fischer and Clarke* [1997], water pressures increase until a local strain build up in the ice is released resulting in an increased sliding rate (possibly at a critical bed separation threshold whereby basal drag is reduced and the glacier speeds up). We suggest that this separation threshold is reached on a diurnal basis at Haut Glacier d'Arolla when water pressures are rising rapidly. Once the strain release has occurred, relaxation takes place and sliding velocities decrease despite the higher water pressures. The strain release could result from the failure of a "sticky spot" resulting in a subsequent stress configuration that is more stable and reduces basal sliding [*Kavanaugh and Clarke*, 2001].

[40] To investigate the extent to which the observed diurnal speed up in the lower glacier could be driven by localized reductions in basal drag in the vicinity of two previously identified subglacial channels, three-dimensional

modeling of glacier flow was undertaken. Model results indicate that basal shear traction requires reduction over a substantially larger area of the bed, up to a distance of about 140 m away from the easterly channel than the lateral excursions of high water pressure observed in 1993 [*Hubbard et al.*, 1995]. The key implication is that significant variations in diurnal velocity will only result when reductions in basal drag occur across an extensive area of the glacier bed. These findings corroborate the field observations of *Iken and Bindschadler* [1996, p. 104], who state that "the subglacial water pressure can affect the sliding velocity only if it acts on a large proportion of the glacier bed (and not just in the vicinity of a few channels)." *Balise and Raymond*'s [1985] two-dimensional theoretical modeling further substantiates this result since they found basal perturbations of 5 to 10 ice thicknesses (H) had maximum impact on the surface velocity response. Although limited to an idealized flow line geometry with a Newtonian linear rheology which ignores transverse stress gradients, their analysis corroborates the three-dimensional modeling presented here insofar as an extensive transverse ($\sim$560 m $\sim 5H$ at row 400) and longitudinal ($\sim$1500 m $\sim 12H$ along the decoupled channels) zone requires a significant reduction in drag to induce the peak subdiurnal velocities observed.

[41] These results imply that glaciers will show significant and regular variations in diurnal velocity when diurnally varying water inputs are delivered to either (1) a hydraulically inefficient distributed system (e.g., at row 800) or (2) a channelized system (e.g., at row 400) with many subglacial channels in which lateral propagation of high basal water pressures adjacent to the channels occurs across a large area of the glacier bed. Where diurnal variations in glacier flow velocities are not evident, this most likely reflects either (1) highly subdued or nonexistent (e.g., in winter) diurnal variations in water inputs or (2) a channelized subglacial drainage system with few large and efficient channels from which lateral excursions of meltwater are spatially limited.

[42] The precise spatial configuration of areas of low drag necessary to induce enhanced basal motion remains unclear. However, the results presented from Haut Glacier d'Arolla clearly suggest that while short-term speed up events are intimately linked to the hydraulic structure of the subglacial drainage system, such speedups are only possible when basal drag is reduced over a large area of the bed. Future modeling programs are needed to investigate more rigorously the extent to which changing configurations of basal shear traction in response to hydrological forcing will impact on ice dynamics at a variety of spatial and temporal scales. Such modeling must address the link between complex temporal and spatial variations in basal water pressure (and thus basal drag) and sliding since the current results suggest that the search for a simple sliding law relating effective pressure to velocity may be inappropriate, at least over short timescales.

[43] **Acknowledgments.** This research was supported by Natural Environment Research Council (NERC) fellowship GT3/93/AAPS/1 (Nienow), NERC grant GR3/8114, NERC studentship GT4/93/6/P (Mair), a Royal Society Grant (Nienow) and Royal Society and Royal Society of Edinburgh Fellowships (Hubbard). M. Nielsen, M. Forster, and D. Clutterbuck provided field assistance, and Grande Dixence SA, Y. Bams, A. Duncan, P. and B. Bournissen, and V. Anzevui provided logistical support. The authors wish to thank two anonymous referees, the Editor, Robert Anderson, and Associate Editor, Garry Clarke, for constructive and insightful reviews and H. Blatter, S. Sugiyama, H. Gudmundsson, and R. Hindmarsh for helpful discussions.

References

Balise, H. J., and C. F. Raymond (1985), Transfer of basal sliding variations to the surface of a linearly viscous glacier, *J. Glaciol.*, *31*(109), 308–318.

Blatter, H. (1995), Velocity and stress fields in grounded glaciers: a simple algorithm for including deviatoric stress gradients, *J. Glaciol.*, *41*(138), 333–344.

Blatter, H., G. K. C. Clarke, and J. Colinge (1998), Stress and velocity fields in glaciers: part II. Sliding and basal stress distribution, *J. Glaciol.*, *44*(148), 457–466.

Colinge, J., and H. Blatter (1998), Stress and velocity fields in glaciers: Part I. Finite-difference schemes for higher-order glacier models, *J. Glaciol.*, *44*(148), 448–456.

Echelmeyer, K. A., and B. Kamb (1986), Stress-gradient coupling in glacier flow: II. Longitudinal averaging in the flow response to small perturbations in ice thickness and surface slope, *Glaciol, J.*, *32*(111), 285–298.

Fischer, U. H., and G. K. C. Clarke (1997), Stick-slip sliding behaviour at the base of a glacier, *Ann. Glaciol.*, *24*, 390–396.

Gordon, S., M. Sharp, B. Hubbard, C. Smart, B. Ketterling, and I. Willis (1998), Seasonal reorganization of subglacial drainage system of Haut Glacier d'Arolla, Valais, Switzerland, inferred from measurements in boreholes, *Hydrol. Processes*, *12*, 105–133.

Gudmundsson, G., A. Iken, and M. Funk (1997), Measurements of ice deformation at the confluence area of Unteraargletscher, Bernese Alps, Switzerland, *J. Glaciol.*, *43*(145), 548–556.

Harbor, J. M., M. Sharp, L. Copland, B. Hubbard, P. Nienow, and D. Mair (1997), The influence of subglacial drainage conditions on the velocity distribution within a glacier cross-section, *Geology*, *25*, 739–742.

Holmlund, P., and R. L. Hooke (1983), High water pressure events in moulins, Storglaciären, Sweden, *Geogr. Ann.*, *65A*, 263–270.

Hooke, R. L., T. Laumann, and J. Kohler (1990), Subglacial water pressures and the shape of subglacial conduits, *J. Glaciol.*, *36*(122), 67–71.

Hubbard, A., H. Blatter, P. Nienow, D. Mair, and B. Hubbard (1998), Comparison of a three-dimensional model for glacier flow with field data from Haut Glacier d'Arolla, Switzerland, *J. Glaciol.*, *44*(147), 368–378.

Hubbard, B., M. Sharp, I. Willis, M. Nielsen, and C. Smart (1995), Borehole water-level variations and the structure of the subglacial drainage system of Haut Glacier d'Arolla, Valais, Switzerland, *J. Glaciol.*, *41*(139), 572–583.

Iken, A. (1974), Velocity fluctuations of an Arctic valley glacier: A study of the White Glacier, Axel Heiberg Island, Canadian Arctic Archipelago, *Axel Heiberg Isl. Res. Rep. Glaciol. 5*, McGill Univ., Montreal, Que., Canada.

Iken, A. (1981), The effect of the subglacial water pressure on the sliding velocity of a glacier in an idealized numerical model, *J. Glaciol.*, *27*(97), 407–421.

Iken, A., and R. A. Bindschadler (1986), Combined measurements of subglacial water pressure and surface velocity of the Findelengletscher, Switzerland: Conclusions about drainage system and sliding mechanism, *J. Glaciol.*, *32*(110), 101–119.

Iken, A., H. Röthlisberger, A. Flotron, and W. Haeberli (1983), The uplift of Unteraargletscher at the beginning of the melt season: A consequence of water storage at the bed?, *J. Glaciol.*, *29*(101), 28–47.

Jansson, P. (1995), Water pressure and basal sliding on Storglaciaren, northern Sweden, *J. Glaciol.*, *41*(138), 232–246.

Kamb, B. (1987), Glacier surge mechanism based on linked cavity configuration of the basal water conduit system, *J. Geophys. Res.*, *92*(B9), 9083–9100.

Kavanaugh, J. L., and G. K. C. Clarke (2001), Abrupt glacier motion and reorganization of basal shear stress following the establishment of a connected drainage system, *J. Glaciol.*, *47*(158), 472–480.

Mair, D., P. Nienow, I. Willis, and M. Sharp (2001), Spatial patterns of glacier motion during a high velocity event: Haut Glacier d'Arolla, Switzerland, *J. Glaciol.*, *47*(156), 9–20.

Mair, D., M. Sharp, and I. Willis (2002), Evidence for basal cavity opening from analysis of surface uplift during a high-velocity event: Haut Glacier d'Arolla, Switzerland, *J. Glaciol.*, *48*(161), 208–216.

Mair, D., I. Willis, B. Hubbard, U. Fischer, P. Nienow, and A. Hubbard (2003), Hydrological controls on patterns of surface, internal and basal motion during three "spring events": Haut Glacier d'Arolla, Switzerland, *J. Glaciol.*, *49*(167), 555–567.

Nienow, P. W. (1993), Dye tracer investigations of glacier hydrological systems, Ph.D. dissertation, Univ. of Cambridge, Cambridge, U.K.

824 Nienow, P., M. Sharp, and I. Willis (1996), Velocity-discharge relationships
825 derived from dye-tracer experiments in glacial meltwaters: Implications
826 for subglacial flow conditions, *Hydrol. Processes*, *10*, 1411–1426.
827 Nienow, P. W., M. J. Sharp, and I. C. Willis (1998), Seasonal changes in the
828 morphology of the subglacial drainage system, Haut Glacier d'Arolla,
829 Switzerland, *Earth Surf. Processes Landforms*, *23*(9), 825–843.
830 Raymond, C. F. (1987), How do glaciers surge? A review, *J. Geophys. Res.*,
831 *92*(B9), 9121–9134.
832 Richards, K. S., M. Sharp, N. Arnold, A. Gurnell, M. Clark, M. Tranter,
833 P. Nienow, G. Brown, I. Willis, and W. Lawson (1996), An integrated
834 approach to studies of glacier hydrology and water quality: Field
835 and modeling studies at the Haut Glacier d'Arolla, Switzerland, *Hydrol.*
836 *Processes*, *10*, 479–508.
837 Sharp, M., K. Richards, I. Willis, N. Arnold, P. Nienow, W. Lawson, and
838 J. L. Tison (1993), Geometry, bed topography and drainage system
839 structure of the Haut Glacier d'Arolla, Switzerland, *Earth Surf. Processes*
840 *Landforms*, *18*(6), 557–571.
841 Willis, I. C. (1995), Intra-annual variations in glacier motion: A review,
842 *Prog. Phys. Geog.*, *19*(1), 61–106.

844 D. M. Chandler and B. P. Hubbard, Centre for Glaciology, Institute of
845 Earth Studies, University of Wales, Aberystwyth SY23 3DB, UK.
846 A. L. Hubbard and P. W. Nienow, School of Geosciences, University of
847 Edinburgh, Drummond Street, Edinburgh EH8 9XP, UK. (pnienow@
848 geo.ed.ac.uk)
849 D. W. F. Mair, Department of Geography and Environment, University of
850 Aberdeen, Elphinstone Road, Aberdeen AB24 3UF, UK.
851 M. J. Sharp, Department of Earth and Atmospheric Sciences, University
852 of Alberta, Edmonton, Alberta, Canada T6G 2H4.
853 I. C. Willis, Department of Geography, University of Cambridge,
854 Downing Place, Cambridge CB3 3EN, UK.